

# **Field Visualization by Image Processing**

## **Image refining and field characteristics**

Marinova, I. <sup>\*1</sup>, Endo, H. <sup>\*2</sup>, Hayano, S. <sup>\*2</sup> and Saito, Y. <sup>\*2</sup>

\*1 Department of Electrical Apparatus, Technical University of Sofia, Sofia-1756, Bulgaria  
Tel: +359-2-965-3873 / FAX: +359-2-962-4196  
E-mail: iliana@vmei.acad.bg

\*2 Faculty of Engineering, Hosei University, 3-7-2 Kajino, Koganei, Tokyo 184-8584, Japan

**Abstract:** The purpose of this article is to apply the image processing technique for visualization of electromagnetic fields. An inverse approach has been developed. The refining, reconstruction and repairing of the images are formulated as an inverse problem. For the image color model, the Poisson equation with open boundary condition is imposed. The color source densities have been evaluated from the color distributions for electromagnetic field data set. The Generalized Vector Sampled Pattern Matching method is applied to solve an ill posed linear system of equations for the corresponding inverse problem. The new color distributions is generated and visualized using the obtained color source densities. With the proposed inverse approach the quality of the images can be essentially improved. Utilizing the color source density distribution, the color distribution of the various field characteristics could be obtained. This article collects several examples for electromagnetic field visualization of the most commonly used sensors.

**Keywords:** Image processing, Electromagnetic field, Visualization, Inverse Problem

## **1. Introduction**

Visualization of electromagnetic fields and processes is very important for investigation and design of electromagnetic devices. The field distribution is required solving many identification, NDT or EMC problems. In many cases the available field data set is insufficient or it is obtained in some limited region. Using such data the visualization of field distribution leads to poor and damaged images.

In order to refine the images, recently, we proposed an approach using formulation and solution of inverse problem over the image (e.g., Marinova et al., 2001). The available field data set is visualized and the image obtained is processed. The image is considered as a 2D-distribution of color components – Red, Green, and Blue (RGB). The 2D-Poisson equation is imposed to be satisfied by each of RGB color components with homogeneous open boundary conditions. In order to evaluate the color component distribution, we determine the color source densities distribution utilizing the Green functions. The inverse problem for color source determination is formulated. The Generalized Vector Sampled Pattern Matching (GVSPM) method is applied to solve the composed ill posed linear system of equations (e.g., Sekijima et al., 2001). New visualization of the color distribution is carried out from the evaluated color sources. Utilizing the RGB color source density distribution, we can determine the color component distribution, which corresponds to the flux density distribution of the system under consideration. In such case, the color distribution of the various field characteristics could be obtained and examined. Several visualization examples

demonstrate versatility and applicability of the proposed inverse approach for field visualization as well as for image processing.

## 2. Color Source Densities

The image colors are considered as a 2D-distribution of color components – RGB. A pixel-oriented strategy has been utilized. The 2D-Poisson equation is imposed to be satisfied by each of RGB color components with homogeneous open boundary conditions

$$\nabla^2 \mathbf{A} = -\sigma \quad (1)$$

where  $\mathbf{A}$  and  $\sigma$  are the any of the color components RGB and color source densities, respectively. The color component  $A$  can be represented by the appropriate Green function  $G$  over image pixels

$$A = \frac{1}{4\pi} \int_s \sigma G dS . \quad (2)$$

In order to determine the color component source densities, we compose a system of equations

$$\mathbf{CX} = \mathbf{Y} , \quad (3)$$

where  $\mathbf{C}$ ,  $\mathbf{Y}$  and  $\mathbf{X}$  are the  $n$  by  $m$  system matrix,  $n$ -th order column vector of the color component and  $m$ -th order column vector of unknown color source densities, respectively. To refine and improve the image, the color components as well as color source densities have to be determined in terms of the  $x$ - and  $y$ - pixels of the target area. The red, green and blue color components are distinctly processed. For each of them the damaged area is extracted and systems of equations (3) in each of the color components are composed. Caused by the extracted damaged area, the number of unknowns in (3)  $m$  is much larger than number of equations  $n$ . The RGB systems of equations become linear but ill posed.

Thus, the inverse problem for color source determination is formulated. In order to solve the RGB systems of equations (3), the GVSPM is applied. The color source densities are determined. The new visualization of the color distributions is carried out from the evaluated color source densities. Because of the solution error of the systems of equations, it is difficult to obtain the exact results. Quality of the reconstructed image is estimated by means of correlation factor. The high quality image could be obtained by organizing iterative procedure.

During visualization of fields when the potential field distribution is considered, the RGB color distribution of the image corresponds to the potential distribution of the field. Applying the relation between vector potential  $\mathbf{A}$  and flux density  $\mathbf{B}$  over the pixels of the image

$$\mathbf{B} = \nabla \times \mathbf{A} , \quad (4)$$

we can obtain the RGB color flux density distribution of the field under consideration. Also, the components of the color flux densities are determined utilizing the color source densities  $\sigma$

$$B_x = \int_s \sigma d_x dS , \quad (5)$$

$$B_y = \int_s \sigma d_y dS , \quad (6)$$

where the  $d_x$  and  $d_y$  represent the geometrical relations between pixels for corresponding components of the flux density. In matrix form (5) and (6) are expressed by

$$\mathbf{B}_x = \mathbf{D}_x \sigma , \quad (7)$$

$$\mathbf{B}_y = \mathbf{D}_y \sigma , \quad (8)$$

where  $\mathbf{D}_x$  and  $\mathbf{D}_y$  are matrix with  $d_x$  and  $d_y$  elements, respectively.

Thus, if the mathematical model of the processes, that are visualized, is applied to the corresponding image during image processing, the different characteristics of these processes can be obtained.

### 3. Applications

The inverse problem formulated above has been applied for image processing along with visualization of the field distribution of electromagnetic devices.

The magnetic field distribution of sensor coil has been studied. The coil is of circular shape. The inner diameter is  $r_1 = 0.01$  m, the outer diameter  $r_2 = 0.03$  m and height is  $h = 0.04$  m. The magnetic field under consideration is axisymmetrical and can be easily visualized using different visualization tools.

The magnetic field distribution of the linear sensor composed of ferromagnetic core with dimensions  $0.020 \times 0.020$  m, height  $h_1 = 0.050$  m and coil with inner and outer dimensions  $d_1 = 0.024$  m,  $d_2 = 0.054$  m and height  $h_2 = 0.030$  m has been investigated. The magnetic field can be considered as 2D-plane.

#### 3.1 Image refining

When the image available is damaged or corrupted, it is difficult to analyze it properly. In order to refine or repair the image, we apply the proposed inverse approach. Figs. 1(a) and (b) show the original (a) and damaged (b) images of magnetic field distribution of the investigated sensor coil, respectively. The damage part is 5% of the entire image, and also low resolution. The systems of equations (3) were composed and solved for each of the three-RGB color components of the damaged image. In this case, we employ the Green function in cylindrical coordinates, expressed by

$$G = \frac{1}{2\pi} \sqrt{\frac{\rho_M}{\rho_Q}} \left[ \left( \sqrt{\frac{2}{k}} - k \right) K(k) - \frac{2}{k} E(k) \right]. \quad (9)$$

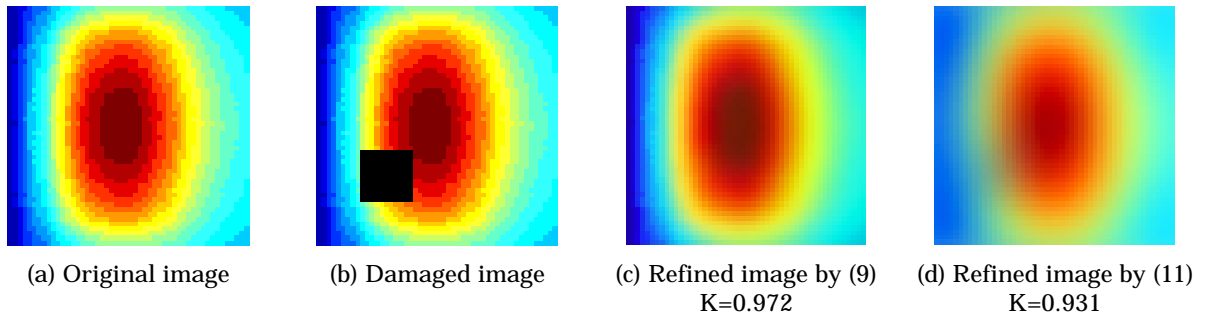


Fig. 1 Original and damaged images of magnetic field distribution of the sensor coil.

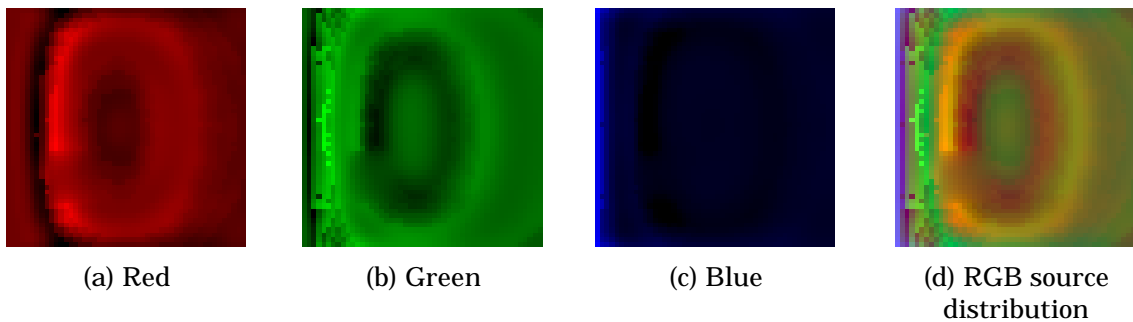


Fig. 2 Color source density distributions of coil sensor.

The module  $k$  in (9) is

$$k^2 = \frac{4\rho_Q\rho_M}{(\rho_Q + \rho_M)^2 + (z_Q - z_M)^2}, \quad (10)$$

and  $K(k)$  and  $E(k)$  are the complete elliptic integrals from first and second kind, respectively;  $\rho_Q, \rho_M$  are the radial coordinates and  $z_Q, z_M$  are the axial coordinates of the pixels of the color component  $A$  and the pixel of the current integration, respectively.

The damaged area was extracted. The solutions of the systems represent the red, green and blue color source densities over image including damage region, shown in Fig. 2. The new visualization of the color distribution is carried out from the evaluated color sources. As a result, we have obtained the refined image. Fig.1(c) shows the result. The correlation coefficient between original and refined images is 0.972. Fig. 1(d) shows the refined image obtained by utilizing the Green function in Cartesian coordinates, expressed by

$$G = \frac{1}{2\pi} \ln \frac{1}{r}. \quad (11)$$

The correlation factor is 0.931. The results in Fig. 1 reveal that the visualized field by axisymmetrical formulation in (9) is capable of providing the better results in terms of the correlation factors. This is caused by the axisymmetrical nature of the magnetic field of the sensor coil under consideration.

Figs. 3(a) and 3(b) show the original and damaged images of magnetic field distribution of the core-coil sensor, respectively. Applying our approach, the systems of equations (3) were solved for the three-RGB color components of the damaged image. In this case, as the magnetic field could be considered as a plane, we employ the Green in 2D Cartesian coordinates, expressed by (11). The RGB color source density distribution is shown in Fig. 4. In Fig. 3(c) is shown the refined image. The calculated correlation factor is  $K=0.828$ .

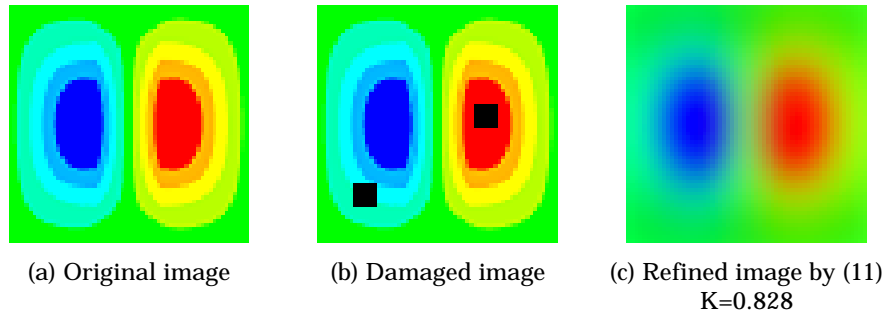


Fig. 3 Original and damaged images of magnetic field distribution of core-coil sensor

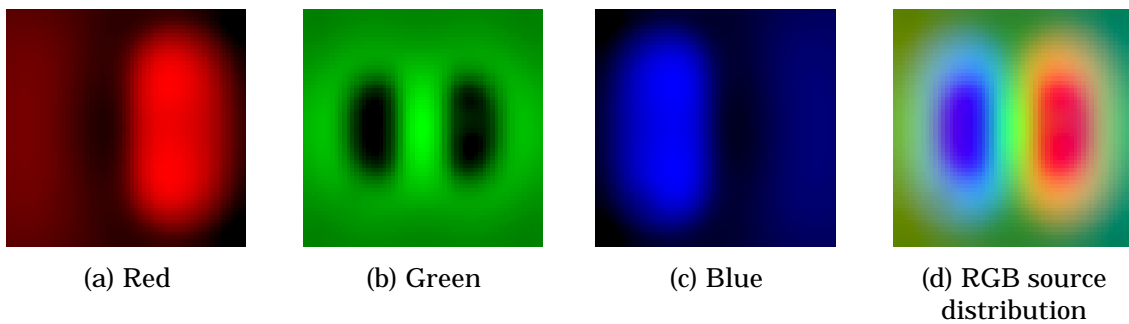


Fig. 4 Color source density distributions of core-coil sensor.

Analyzing the result presented in Figs 1-4 it was found that during the image processing in order to refine the images the fairly good result could be obtained utilizing the expressions that model the visualized fields.

### 3.2 Field characteristics determination

Considering potential distribution of the magnetic field and utilizing the RGB color source density distribution, we can obtain the color flux density distribution by (4)-(8). In case of cylindrical coordinate system the elements  $d_x$  and  $d_y$  of the matrix  $\mathbf{D}_x$  and  $\mathbf{D}_y$  are

$$d_x = \frac{1}{2\pi} \frac{z_Q - z_M}{\rho_Q \sqrt{(\rho_Q + \rho_M)^2 + (z_Q - z_M)^2}} \left[ -K(k) + \frac{\rho_Q^2 + \rho_M^2 + (z_Q - z_M)^2}{(\rho_Q - \rho_M)^2 + (z_Q - z_M)^2} E(k) \right], \quad (12)$$

$$d_y = \frac{1}{2\pi} \frac{1}{\sqrt{(\rho_Q + \rho_M)^2 + (z_Q - z_M)^2}} \left[ K(k) + \frac{\rho_M^2 - \rho_Q^2 + (z_Q - z_M)^2}{(\rho_Q - \rho_M)^2 + (z_Q - z_M)^2} E(k) \right]. \quad (13)$$

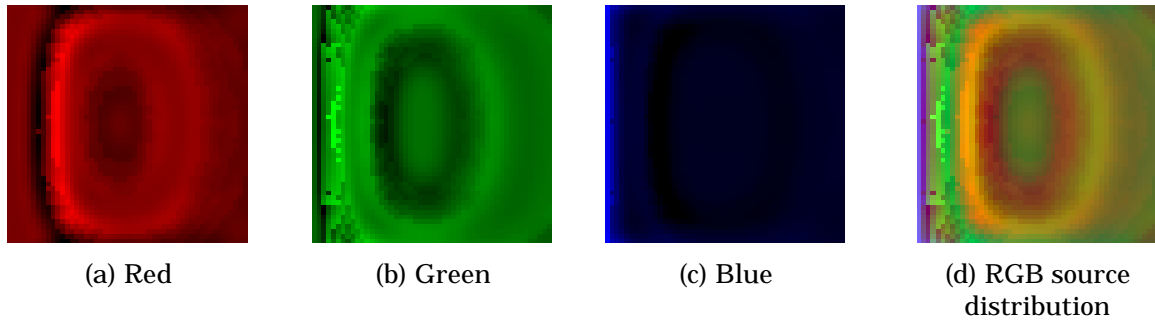


Fig. 5 Color source densities distribution of the coil sensor

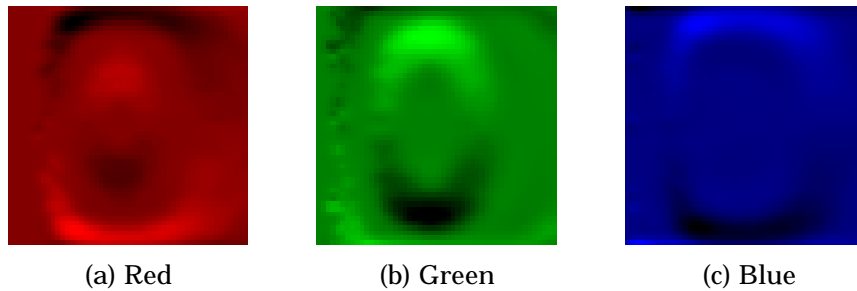


Fig. 6 X-components of the RGB color flux density distribution of coil sensor

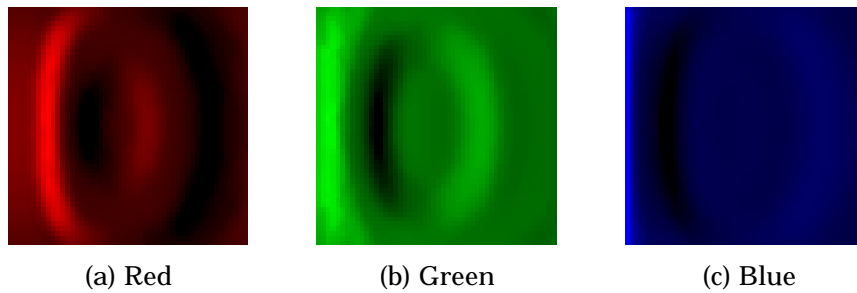


Fig. 7 Y-components of the RGB color flux density distribution of coil sensor

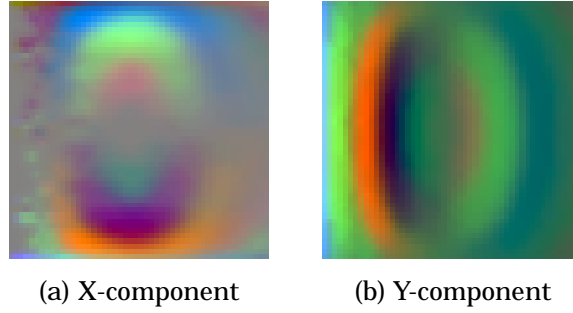


Fig. 8 X- and Y-components of the color flux density distribution of coil sensor

In case of Cartesian coordinate system the elements  $d_x$  and  $d_y$  of the matrix  $\mathbf{D}_x$  and  $\mathbf{D}_y$  are

$$d_x = \frac{1}{2\pi} \frac{y_M - y_Q}{(x_M - x_Q)^2 + (y_M - y_Q)^2}, \quad (14)$$

$$d_y = -\frac{1}{2\pi} \frac{x_M - x_Q}{(x_M - x_Q)^2 + (y_M - y_Q)^2}, \quad (15)$$

In (12)-(15)  $x$  and  $y$  are the coordinates of the current pixel  $M$  and the pixel of observation  $Q$ .

Utilizing the obtained RGB color source densities distributions for coil sensor shown in Fig. 5, we can determine the X- and Y- components of the RGB color flux density distributions, presented in Fig. 6 and Fig.7. As the magnetic field is axisymmetrical the expression (12)-(13) are used. The X- and Y-components of the color flux density distributions determined by image processing of the potential distribution of the coil sensor are shown in Fig.8. The color flux density distributions correspond to the flux density distributions of the visualized magnetic filed.

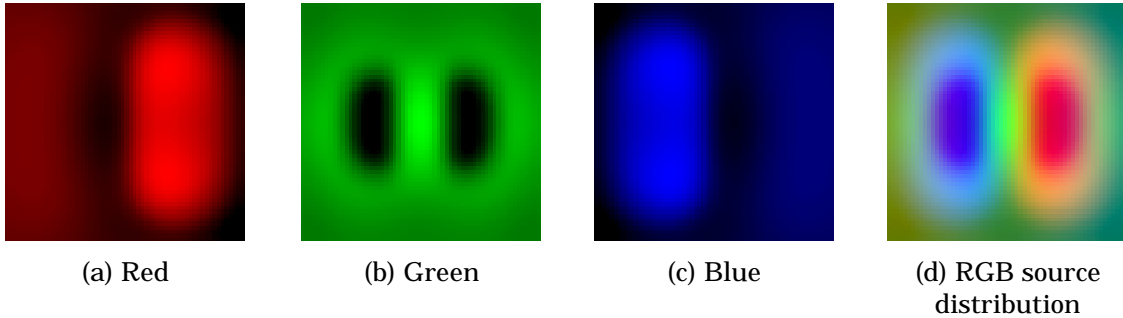


Fig. 9 Color source densities distribution of the core-coil sensor

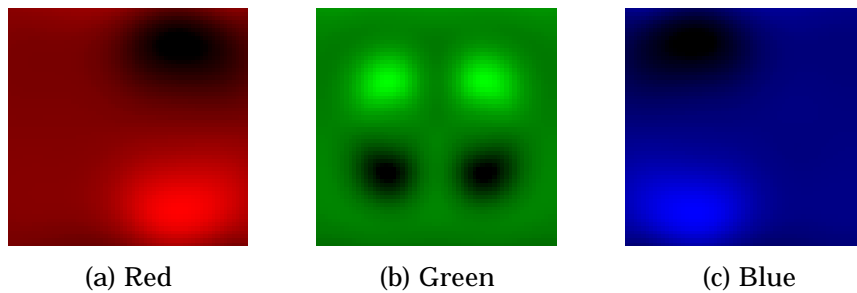


Fig. 10 X-components of the RGB color flux density distribution of the core-coil sensor

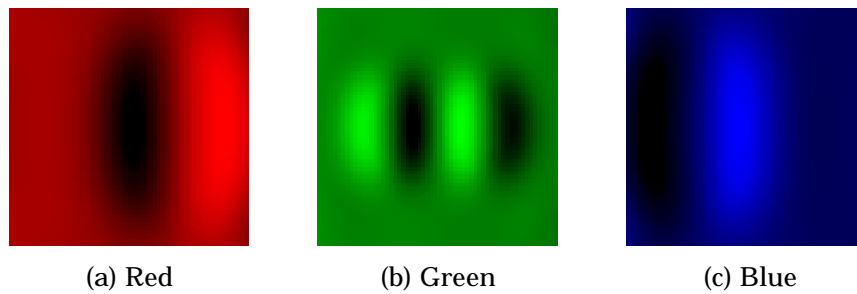


Fig. 11 Y-components of the RGB color flux density distribution of core-coil sensor.

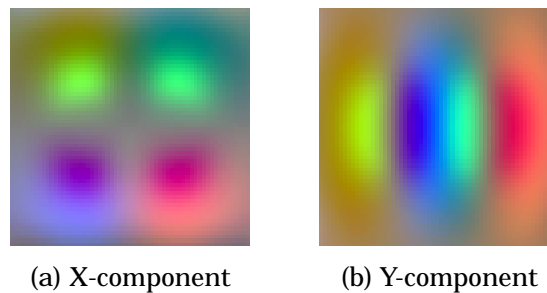


Fig. 12 X- and Y-components of the color flux density distribution of core-coil sensor

For the core coil sensor, the RGB color flux density distributions are determined by color source density distributions shown in Fig. 9. The X- and Y- components of color flux density distributions are presented in Fig. 10 and Fig.11. As the magnetic field is 2D-plane, the expressions (14)-(15) are used. The X- and Y-components of the color flux density distributions determined by image processing of the potential distribution of the core-coil sensor are shown in Fig.12.

## 4. Conclusion

In this article, we have applied the inverse approach for image refining. The color source densities distributions have been determined by solving of the image inverse problem. The new RGB color distributions have been generated. With appropriate selection of the Green function, it is possible essentially to improve the quality of the image. Thus, it has been found that if the relations of the mathematical model describing the visualized field are applied to the image during the image processing, the various field characteristics could be obtained. Thereby, from potential distribution of magnetic field, it is possible to visualize the flux density distribution.

## References

- Marinova I., Endo H., Hayano S., Saito Y., 2001, "Image reconstruction for electromagnetic field visualization by an inverse problem solution", Applied Electromagnetics and Mechanics, T. Takagi and M. Uesaka (eds.) ©2001 JSAEM, 699
- Sekijima D., Miyahara S., Hayano S., Saito Y., 2000, "A study on the quasi-3D current estimation," Trans. IEE of Japan, Vol. 120-A, No.10, pp.907-912 (in Japanese).